# Theory of tracking accuracy of laser systems

**Leonid G. Kazovsky**
West Virginia University
Department of Electrical Engineering
Morgantown, West Virginia 26506

**Abstract.** Optical rangefinders, lidars, and laser tracking systems offer new options for a variety of applications. When a laser system operates in a tracking regime, it must continuously estimate target angle coordinates. This purpose may be achieved by means of a quadrant detector (QD) incorporated in the optical receiver. In this paper, performance of the QD-based laser tracker is evaluated theoretically. Angle measurement span, angle estimation bias, and angle estimation variance are analyzed with the emphasis on the quantitative evaluation of the estimation bias and variance. It is shown that the estimation error contains both systematic error (signal-independent bias) and signal-dependent bias. The systematic error is caused by the signal processing circuitry of the receiver; this error is rather large (up to 11.5% of the measurement span), but may be easily cancelled by means of a permanent look-up correction table stored in a ROM (read-only memory). Signal-dependent bias cannot be cancelled with the same technique since it depends on the *a priori* unknown signal intensity. Fortunately, signal-dependent bias decreases when the SNR (signal-to-noise ratio) increases, at a rate proportional to $\sqrt{SNR}$; however, it increases rapidly when the light spot approaches the end of the measurement span. Estimation variance is also evaluated. It is found to decrease when the SNR increases, at a rate roughly proportional to SNR. Estimation variance remains approximately constant as the light spot moves over the measurement span. Thus, the main consequence of the deviation of the light spot from the QD center is the increase of the estimation bias, rather than a change of the estimation variance.

*Keywords: quadrant detectors; lidar; angle estimation; bias and variance evaluation; tracking.*

*Optical Engineering 22(3), 339-347 (May/June 1983).*

## CONTENTS



## 1. INTRODUCTION

Optical rangefinders, lidars, and laser tracking systems offer new options for a variety of applications.[1-3] Laser systems are similar to conventional radar systems[4] in many respects. In particular, two modes of operation of scanning laser systems are generally recognized: search (or surveillance) mode and tracking mode. In the search mode, a lidar scans a prescribed space sector looking for a target. If a target is detected, then it is continuously tracked. Normally, angle tracking is required although sometimes range tracking is also needed. In some cases, surveillance and tracking are performed by different systems; in other cases, the same lidar is used for both surveillance and tracking.[4,5] Target angle tracking implies continuous estimating of the target angle coordinates. This purpose is typically achieved by means of a mosaic sensor[6-8] placed in or near the focal plane of the optical receiver. Frequently, the simplest form of a mosaic sensor is used[8]—quadrant detector (QD). The common approach is to measure the target's position by using the main optical servo system angles, with the quadrant detector serving as the error detector. As a result, the system accuracy is upper-bounded by the quadrant error detector accuracy. A more sophisticated system may use the servo system's tracking error, as measured by the quadrant detector, to refine the target's position estimate supplied by the main optical servo system. In other words, the quadrant detector may be used to perform a measurement of a target's angular position in the optical tracking system's field of view. In this case, the system accuracy may actually approach the quadrant error detector accuracy.

In this paper, performance of the QD-based angular position tracker is evaluated theoretically. Our analysis takes into account the following inaccuracy sources: (a) quantum noise associated with the optical signal field; (b) background noise; (c) noise associated with the photodetector dark current; (d) thermal noise of the photodetector and of the associated electronic circuits. However, performance limitations of the main optical servo system are not taken into account. Therefore, performance measures derived in this paper represent upper bounds to the performance of optical tracking systems. Performance of a practical system may approach these bounds if the system uses the QD-derived signals to measure a target's angular position in the optical

Paper 1880 received May 10, 1982; revised manuscript received Nov. 16, 1982; accepted for publication Nov. 23, 1982; received by Managing Editor Dec. 6, 1982.

tracking system's field of view and/or if the inaccuracy due to the main optical servo system is much smaller than that due to the quadrant detector.

The rest of this paper is organized as follows. Model description and problem statement are given in Sec. 2. Performance of the QD-based tracker is evaluated in Sec. 3. In particular, measurement span, estimation bias, and estimation variance are discussed, with the emphasis on the quantitative evaluation of the estimation bias and variance. For the sake of simplicity, a sinusoidally modulated cw optical signal is assumed through Sec. 3. Finally, Sec. 4 summarizes the main results of this paper.

## 2. MODEL DESCRIPTION AND PROBLEM STATEMENT

Consider a model shown in Fig. 1. This model represents the receiver of an optical tracking system, and operates as follows. The intensity-modulated received beam falls upon the input lens of the receiver. The beam is generated and intensity-modulated by a laser transmitter, not shown in Fig. 1. The beam arrives at the receiver after being reflected by a remote target, which is also not shown in Fig. 1. The input lens of the receiver concentrates the beam into the light spot on the surface of the quadrant detector (QD). The optical filter is placed between the lens and the QD; its purpose is to suppress background radiation. The position of the light spot on the QD surface is given by the vector (x, y). x and y are the x and y coordinates of the spot center; they are identified in Fig. 2. Once the vector (x, y) is estimated, the angles of arrival of the received beam may be computed as follows (Ref. 10, p. 31):

$$\theta_x = \arcsin x/f_c \ ;$$

$$\theta_y = \arcsin y/f_c \ ,$$

where $\theta_x$ and $\theta_y$ are the arrival angles measured from the system optical axis and $f_c$ is the system focal length. Thus, in the rest of this paper we concentrate our efforts on the estimation of the vector (x, y). The estimation is performed as follows. The output currents of the photodetectors are filtered by the bandpass filters tuned to the modulation frequency of the received beam. The output signals of the filters are rectified and then transferred to the data processor for the remaining processing indicated in Fig. 1. The output signals of the data processor are $\hat{x}$(the estimated value of x) and $\hat{y}$ (the estimated value of y). In the following section we analyze the performance of the described system.

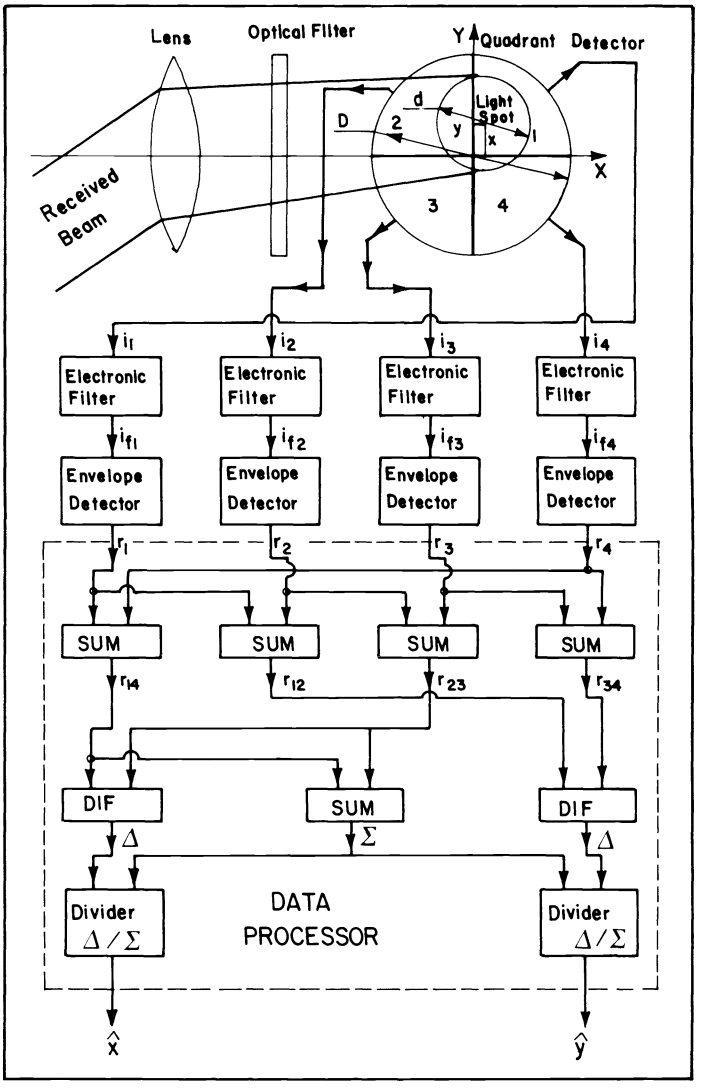


Fig. 1. Layout of receiver of lidar tracker.

## 3. PERFORMANCE EVALUATION

The purpose of the described system is estimation of the target angle. Thus, the performance of the system is characterized by the following parameters: (a) angle measurement span, (b) angle estimation bias, and (c) angle estimation variance. Since angle estimation is accomplished via estimation of the position of the light spot, the parameters (a), (b), and (c) depend uniquely on the receiver optics design and on (d) (x, y) measurement span, (e) (x, y) estimation bias, and (f) (x, y) estimation variance, respectively. Performance measures (d), (e), and (f) are evaluated in the following subsections.

### 3.1. Measurement span

Both x and y can be efficiently estimated provided the following two conditions are satisfied: (a) the entire light spot is located within the QD area; (b) each of the four detectors receives part of the signal energy.

If condition (a) is not satisfied, then a part of the light spot is located outside the QD; this part of the signal energy is lost, with the corresponding performance degradation. If condition (b) is not satisfied, then at least one of the photodetectors receives only background field; this detector contributes no useful information, thus indicating that the system is not efficiently used. Thus, both (a) and (b) must be satisfied. Let us define the system measurement span as a largest

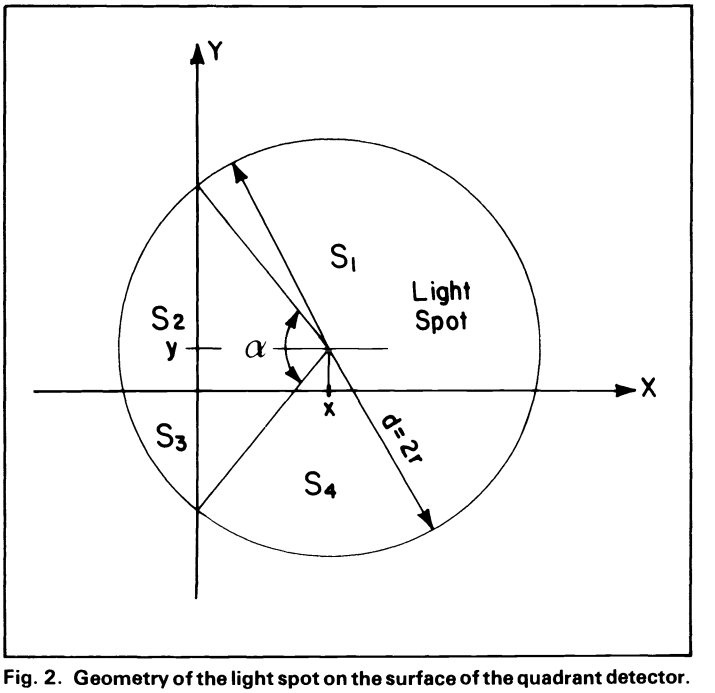


Fig. 2. Geometry of the light spot on the surface of the quadrant detector.

possible x (or y) that does not cause violation of either (a) or (b). A little thought shows that the widest possible span is obtained when

$$d = D/2 , \tag{1}$$

where d is the diameter of the light spot, and D is the diameter of the QD. If expression (1) is satisfied, then the measurement span M is

$$M = d/2 = r = D/4 . \tag{2}$$

In other words, the measurement span is equal to the radius of the light spot r. Unfortunately, the foregoing discussion is too simplified. As we shall see in the following subsections, the measurement span must be limited to a fraction of the spot radius if the measurement bias is to be kept within reasonable limits.

### 3.2. Estimation bias and estimation variance: definitions

Normalized estimation bias and variance in the x-direction are defined as follows:

$$b\hat{x} \triangleq \left[E(\hat{x}|x) - x\right]/r ; \tag{3a}$$

$$\text{var}\,\hat{x} \triangleq \left\{E\left[(\hat{x} - E(\hat{x}))^2|x\right]\right\}/r^2 , \tag{3b}$$

where $E(\cdot)$ denotes mathematical expectation of $(\cdot)$. Estimation bias and variance in the y-direction are defined analogously. Since our estimation device is symmetrical, we will evaluate the bias and the variance in one direction only.

### 3.3. Statistical properties of the estimate: general development

At this point, we must specify a model of the detector's currents. The generally accepted model assumes[9-11] that

$$i_k = \bar{i}_{sk} + \bar{i}_{nk} + i_{nk} , \tag{4}$$

where $i_k$ is the detector current, $\bar{i}_{sk}$ is the average signal current, $\bar{i}_{nk}$ is the average noise current (dc), and $i_{nk}$ is a zero-mean random process—all for the k-th detector. Expression (4) implies that system noises generally have a nonzero mean. Thus, expression (4) reflects the following noises: (a) quantum noise associated with the optical signal field*; (b) background noise*; (c) noise associated with the photodetector dark current*; (d) thermal noise of the photodetector and of the associated electronic circuits.

Note that all the foregoing noises contribute to $i_{nk}$ but only (b) and (c) contribute to $\bar{i}_{nk}$. The signal component $\bar{i}_{sk}$ may be found as follows[9-11]:

$$\bar{i}_{sk} = \frac{\eta q S_k I}{h\nu}\, y(\theta) , \tag{5}$$

where $\eta$ is the quantum efficiency, q is the electron charge, h is the Planck constant, $\nu$ is the light frequency, I is the irradiance of the signal field, $S_k$ is the area of the light spot on the surface of the k-th detector, $y(\cdot)$ is the photodetector angle response, and $\theta$ is the angle of incidence of light on the detector surface. In tracking lidars, $\theta$ is kept small so that $y(\theta) \simeq 1$; consequently, expression (5) yields

$$\bar{i}_{sk} = \frac{\eta q S_k I}{h\nu} . \tag{6}$$

If intensity modulation is used, then

$$I = I_0(1 + m\sin\omega t) , \tag{7}$$

where $I_0$ is the nominal light irradiance, m is the depth of modulation, and $\omega$ is the modulation frequency; sinusoidal modulation was assumed. Substituting expression (7) in (6) yields

$$\bar{i}_{sk} = \bar{i}_s \frac{S_k}{S}(1 + m\sin\omega t) , \tag{8}$$

where

$$\bar{i}_s \triangleq \frac{\eta q I_0 S}{h\nu} \tag{9}$$

is the total signal current, and S is the total area of the light spot. Now, the detector currents are filtered by bandpass filters tuned to the modulation frequency $\omega$ (Fig. 1). Hence,

$$i_{fk} = \bar{i}_s \frac{S_k}{S} m\sin\omega t + i_{fnk} , \tag{10}$$

where $i_{fk}$ and $i_{fnk}$ are the filtered versions of $i_k$ and $i_{nk}$, respectively. Note that the dc components of the system noise and of the signal do not appear in expression (10) since both of them are rejected by the bandpass filters. $i_{fnk}$ is a band-limited white noise process with variance

$$\text{var}\, i_{fnk} = B \cdot N_k , \tag{11}$$

where $N_k$ is the power spectral density of $i_{nk}$, and B is the bandwidth of electronic filters. $N_k$ may be found as follows[8-10]:

$$N_k = N_t + 2q(\bar{i}_{sk} + \bar{i}_d + \bar{i}_b) , \tag{12}$$

where $N_t$ is the power spectral density of the thermal noise due to both the photodetector and the associated electronic circuits, $\bar{i}_d$ is the detector dark current, and $\bar{i}_b$ is the detector current due to background radiation. Expression (12) implies that $i_{nk}$ and, consequently, $i_{fnk}$ are both nonstationary processes since $\bar{i}_{sk}$ varies with time, as indicated by expression (8). In addition, $N_k$ depends on $S_k$ since $\bar{i}_{sk}$ depends on $S_k$. $N_k$ reaches its maximum when $\bar{i}_{sk}$ is equal to its maximum value:

$$\bar{i}_{sk} = \bar{i}_s \cdot (1 + m) . \tag{13}$$

For a worst case analysis, we substitute expression (13) in (12) and expression (12) in (11):

$$\text{var}\, i_{fnk} = B\left[N_t + 2q(\bar{i}_s + \bar{i}_s m + \bar{i}_d + \bar{i}_b)\right] . \tag{14}$$

Since $i_{fk}$ is composed of the sinusoidal signal and of the band-limited noise [see expression (10)], its envelope is a Rician random variable at every given time moment[12]:

$$p(r_k) = \frac{r_k}{\sigma_k^2} \cdot \exp\left[-\frac{r_k^2 + a_k^2}{2\sigma_k^2}\right] \cdot I_0\left(\frac{a_k r_k}{\sigma_k^2}\right) , \qquad r_k > 0 , \tag{15}$$

where $r_k$ is the envelope of $i_{fk}$, $p(r_k)$ is the probability density function (PDF) of $r_k$, $I_0(\cdot)$ is the modified Bessel function of the first kind of zero order, and $a_k$ and $\sigma_k^2$ are defined as follows:

$$a_k \triangleq \bar{i}_s m \frac{S_k}{S} , \tag{16}$$

and

$$\sigma_k^2 \triangleq \text{var}\, i_{fnk} = BN_k . \tag{17}$$

*All noises marked by * manifest themselves as a shot noise in the detector current.

If envelope detectors (Fig. 1) exactly measure signal envelope, then their output signals are $\{r_k\}_{k=1}^4$ whose PDFs are given by expression (15). The moments of $r_k$ are[12]

$$\bar{r}_k = \sigma_k\sqrt{\frac{\pi}{2}}\left[\left(1+\frac{a_k^2}{2\sigma_k^2}\right)\cdot I_0\left(\frac{a_k^2}{4\sigma_k^2}\right) + \frac{a_k^2}{2\sigma_k^2}\cdot I_1\left(\frac{a_k^2}{4\sigma_k^2}\right)\right]\exp\left(-\frac{a_k^2}{4\sigma_k^2}\right) \tag{18}$$

and

$$\text{var } r_k = 2\sigma_k^2 + a_k^2 - \bar{r}_k^2 , \tag{19}$$

where $\bar{r}_k$ is the expectation of $r_k$, and $I_1(\cdot)$ is the modified Bessel function of the first kind of first order. Expressions (18) and (19) may be greatly simplified if

$$a_k^2 \gg \sigma_k^2 . \tag{20}$$

If expression (20) holds true, then (18) and (19) yield, respectively,

$$\bar{r}_k = a_k(1+\beta_k) \tag{21}$$

and

$$\text{var } r_k = \sigma_k^2(1-\beta_k) , \tag{22}$$

where

$$\beta_k \stackrel{\Delta}{=} \sigma_k^2/2a_k^2 . \tag{23}$$

For a worst case analysis, we substitute expression (14) in (17) and then expressions (17) and (16) in (23); the result is

$$\beta_k = \frac{1}{2\text{SNR}}\frac{S^2}{S_k^2} , \tag{24}$$

where the signal-to-noise ratio (SNR) is defined as follows:

$$\text{SNR} \stackrel{\Delta}{=} (\bar{i}_s m)^2/B\left[N_t + 2q(\bar{i}_s + \bar{i}_{sm} + \bar{i}_d + \bar{i}_b)\right] . \tag{24a}$$

Using expression (24) in (20), we see that condition (20) is satisfied if and only if

$$\text{SNR} \gg S^2/S_k^2 . \tag{25}$$

In other words, approximations (21) and (22) may be used for high signal-to-noise ratios if the light spot is located not "too far" from the QD center. If, however, deviation of the light spot is large, then at least one of $S_k$ approaches zero, and expressions (20)–(22) are no longer valid. For instance, when $x = r$ and $y = 0$, both $S_2$ and $S_3$ are zero (see Fig. 1 and Fig. 2). In this case, $a_2 = a_3 = 0$ and expressions (18) and (19) yield, respectively,

$$\bar{r}_2 = \bar{r}_3 = \sigma_2\sqrt{\frac{\pi}{2}} \tag{26}$$

and

$$\text{var } r_2 = \text{var } r_3 = \sigma_2^2\left[2-\sqrt{\frac{\pi}{2}}\right] \simeq 0.75\,\sigma_2^2 , \tag{27}$$

where

$$\sigma_2 = \sigma_3 = B\left[N_t + 2q(\bar{i}_d + \bar{i}_b)\right] . \tag{28}$$

As for $r_1$ and $r_4$, in this case they are identically distributed, and their moments may be found using expressions (21) and (22).

After $\{r_k\}_{k=1}^4$ have been computed, the $\hat{x}$-channel of the data processor (Fig. 1) computes

$$\Sigma \stackrel{\Delta}{=} \sum_{k=1}^{4} r_k \tag{29}$$

and

$$\Delta \stackrel{\Delta}{=} r_{14} - r_{23} = r_1 + r_4 - r_2 - r_3 . \tag{30}$$

Assuming $\{i_{fnk}\}_{k=1}^4$ to be mutually statistically independent, we obtain

$$E(\Sigma) = \sum_{k=1}^{4} E(r_k) , \tag{31}$$

$$\text{var } \Sigma = \sum_{k=1}^{4} \text{var } r_k , \tag{32}$$

$$E(\Delta) = E(r_1) + E(r_4) - E(r_2) - E(r_3) , \tag{33}$$

and

$$\text{var } \Delta = \sum_{k=1}^{4} \text{var } r_k = \text{var } \Sigma . \tag{34}$$

The final step of estimation of x is (Fig. 1)

$$\hat{x} = r\frac{\Delta}{\Sigma} . \tag{35}$$

Our last task is, therefore, evaluation of the moments of $\hat{x}$. Unfortunately, this task is extremely difficult in a general case since it implies determination of the moments of a *nonlinear* function of mutually statistically *dependent* variables $\Delta$ and $\Sigma$. This difficulty may be avoided if

$$x \ll d . \tag{36}$$

Expression (36) implies that the deviation of the light spot from its normal position ($x = 0$, $y = 0$) is small—this condition is frequently satisfied in practical systems. If condition (36) is indeed satisfied, then

$$E(\Delta) \ll E(\Sigma) . \tag{37}$$

Since $\text{var } \Delta = \text{var } \Sigma$ [see (34)], expression (37) implies that the impact of the random fluctuations of $\Delta$ is much more noticeable than that of $\Sigma$. This statement may be illustrated by assuming $E(\Delta) = 0$ and rewriting expression (35) as follows:

$$\hat{x} = r\frac{\text{ran }\Delta}{E(\Sigma) + \text{ran }\Sigma} = r\frac{\text{ran }\Delta}{E(\Sigma)}\cdot\frac{1}{[1 + (\text{ran }\Sigma)/E(\Sigma)]} \simeq r\frac{\text{ran }\Delta}{E(\Sigma)} ; \qquad E(\Delta) = 0 , \tag{38}$$

where ran $\Delta$ and ran $\Sigma$ denote the random zero mean components of $\Delta$ and $\Sigma$, respectively; we have assumed $(\text{ran }\Sigma)/E(\Sigma) \ll 1$, i.e., high signal-to-noise ratio. The foregoing discussion leads us to the follow-

ing *approximate* expression:

$$\hat{x} = r\frac{\Delta}{E(\Sigma)} . \tag{39}$$

We emphasize that expression (39) is only approximation and may lead to underestimation of the variance and of the bias of $\hat{x}$. With the foregoing reservation in mind, let us apply (39) for evaluation of the var $\hat{x}$ and $b\hat{x}$. (Note: expression (39) will be used even if (36) is not satisfied.) Applying the operator of mathematical expectation to expression (39), we obtain

$$E(\hat{x}) = r\frac{E(\Delta)}{E(\Sigma)} = r\frac{E(r_1) + E(r_4) - E(r_2) - E(r_3)}{\sum_{k=1}^{4} \bar{r}_k} , \tag{40}$$

where $\bar{r}_k \triangleq E(r_k)$. If expression (25) holds true, then (21) may be substituted in (40), with the following result (we have used expression (24) for $\beta_k$ and expression (14) for $\sigma_k^2$):

$$E(\hat{x}) = r\hat{x}_1 + r \cdot SNR^{-1} \cdot \left[\left(\frac{S}{S_1} + \frac{S}{S_4}\right)(1 - \hat{x}_1) - \left(\frac{S}{S_2} + \frac{S}{S_3}\right)(1 + \hat{x}_1)\right] + \epsilon , \tag{41}$$

where $\epsilon$ denotes higher order terms, which are proportional to $SNR^{-m}(m \geq 2)$, and $\hat{x}_1$ is defined as follows:

$$\hat{x}_1 \triangleq \frac{(S_1 + S_4) - (S_2 + S_3)}{S} . \tag{42}$$

Note that $\hat{x}_1$ depends neither on the received signal nor on the accompanying noises; thus, $\hat{x}_1$ represents a signal-independent component of $E(\hat{x})$. Let us first evaluate the accuracy of expression (42) and then proceed to the signal-dependent bias and variance.

Assuming a circular light spot, we may use simple geometric formulas:

$$S_2 + S_3 = \frac{d^2}{8}\left(\frac{\pi\alpha}{180} - \sin\alpha\right) ; \tag{43}$$

$$S_1 + S_4 = \frac{\pi d^2}{4} - (S_2 + S_3) ; \tag{44}$$

$$\alpha = 2\arccos\frac{2x}{d} ; \tag{45}$$

$$S = \pi d^2/4 ; \tag{46}$$

where $\alpha$ is indicated in Fig. 2. Figure 3 shows $\hat{x}_1$ versus $x/r$; the plot was computed using expressions (42)–(46). Inspection of Fig. 3 reveals that although $\hat{x}_1$ generally follows x, the curve is noticeably nonlinear.

### 3.4. Systematic error, or signal-independent bias

Figure 4 shows $b_1$ versus $x/r$, where $b_1$ is the systematic error:

$$b_1 \triangleq \hat{x}_1 - x/r . \tag{47}$$

We recall that r is the radius of the light spot. Inspection of Fig. 4 reveals that the systematic error is always positive; further, the maximum systematic error is 0.115, i.e., 11.5% of the measurement span.

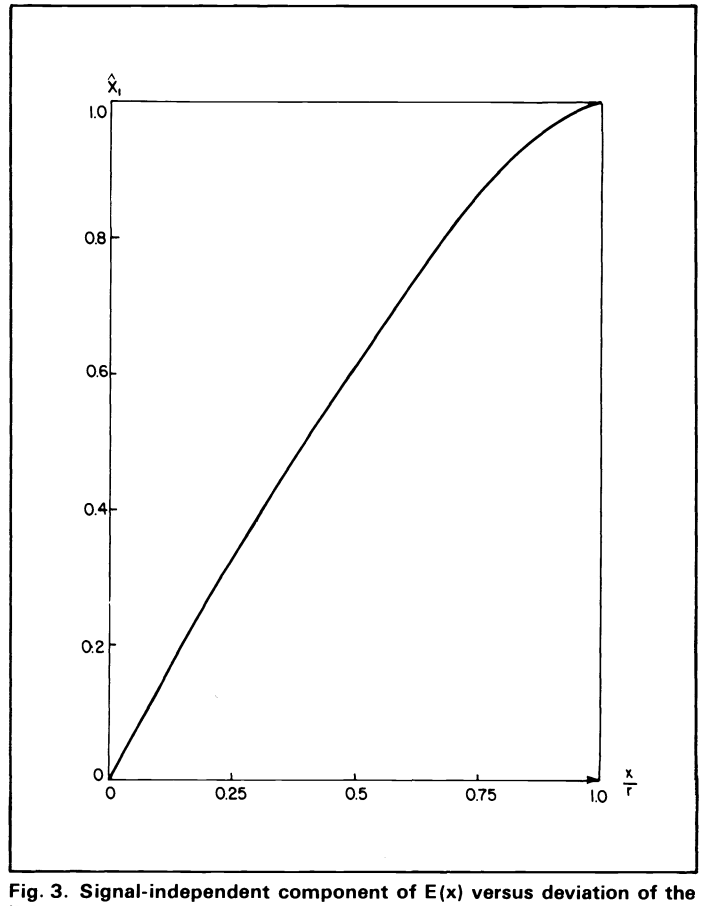


**Fig. 3. Signal-independent component of E(x) versus deviation of the light spot.**

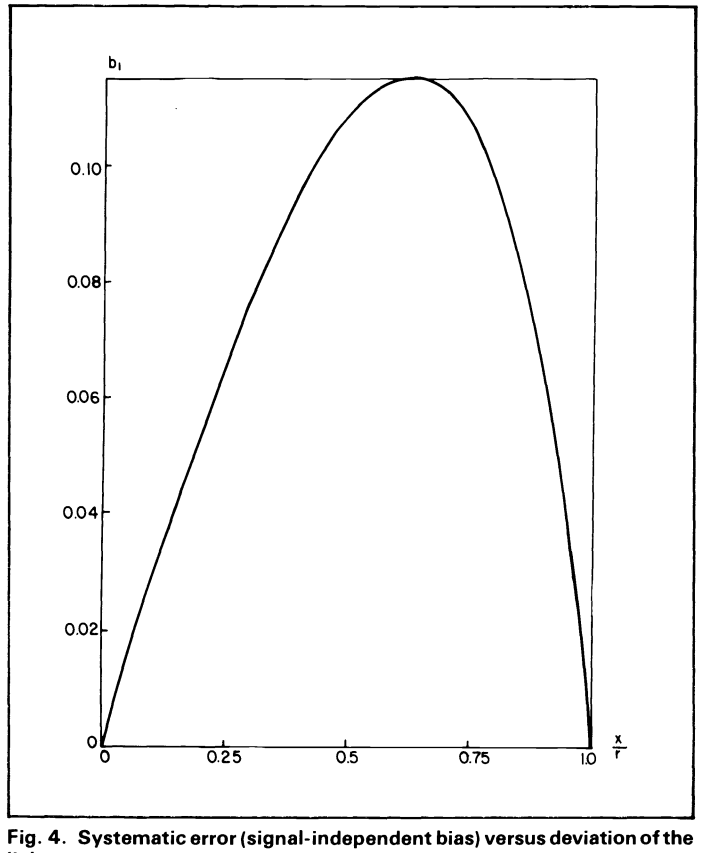


**Fig. 4. Systematic error (signal-independent bias) versus deviation of the light spot.**

Numerical analysis shows that the average mean squared value of $b_1$ is 0.0832, i.e., 8.32% of the measurement span. The foregoing error is predictable and signal-independent. Therefore, it may be corrected.* One way to cancel a systematic error is to store a permanent look-up correction table in a ROM (read-only memory)—a relatively simple and inexpensive solution.

Now, let use return to expressions (40) and (41). In addition to the easily corrected systematic error, they contain a signal-dependent bias.

### 3.5. Signal-dependent bias

The signal-dependent bias is defined as follows:

$$b_2 \triangleq E\left(\frac{\hat{x}}{r}\right) - \hat{x}_1 \ . \tag{48}$$

In this subsection we derive an expression which allows us to compute $b_2$ (and later b) for an arbitrary x. We assume a circular light spot located on the x-axis. Then it follows from expressions (43)–(46) that

$$\alpha = 2\arccos\frac{x}{r} \ , \tag{49}$$

$$S_2^1 = 0.25\left(\frac{\pi\alpha[\text{deg}]}{180} - \sin\alpha\right) = 0.25(\alpha[\text{rad}] - \sin\alpha) \ , \tag{50}$$

and

$$S_1^1 = \frac{\pi}{2} - \frac{S_2}{r^2} \ , \tag{51}$$

where

$$S_2^1 \triangleq \frac{S_2}{r^2} = \frac{S_3}{r^2} \ , \text{ and } S_1^1 \triangleq \frac{S_1}{r^2} = \frac{S_4}{r^2} \ .$$

Combining expressions (14), (16), and (17), we obtain

$$G_k \triangleq \frac{a_k^2}{4\sigma_k^2} = 0.25 \cdot \text{SNR} \cdot S_k^2/S^2$$

$$= 0.25 \cdot \text{SNR} \cdot (S_k^1/\pi)^2 \ , \qquad k = 1,2,3,4 \ . \tag{52}$$

It follows from expression (18) that

$$\bar{r}_k^1 = \left[(1 + 2G_k) \cdot I_0(G_k) + 2G_k \cdot I_1(G_k)\right]\exp(-G_k) \ , \tag{53}$$

where

$$\bar{r}_k^1 \triangleq \bar{r}_k/\sigma_k\sqrt{\pi/2} \ .$$

Further, it follows from expression (40) that

$$E(\hat{x}/r) = \frac{\bar{r}_1^1 - \bar{r}_2^1}{\bar{r}_1^1 + \bar{r}_2^1} \tag{54}$$

since $\bar{r}_1^1 = \bar{r}_4^1$ and $\bar{r}_2^1 = \bar{r}_3^1$. Now, according to expression (42),

$$\hat{x}_1 = 2\frac{S_1^1 - S_2^1}{S^1} = 2(S_1^1 - S_2^1)/\pi \ , \tag{55}$$

where $S^1 \triangleq S/r^2 = \pi$. Finally, expressions (48), (54), and (55) allow one to compute

*One must remember that a nonlinear correction of the systematic error can increase the signal-dependent bias and variance.

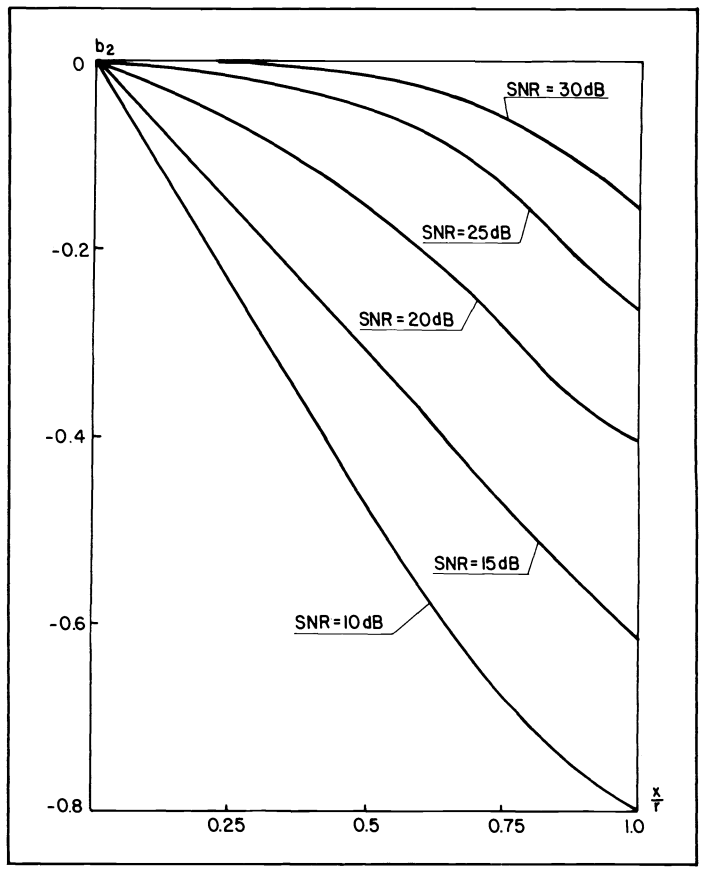


**Fig. 5. Signal-dependent bias versus deviation of the light spot.**

$$b_2 = E(\hat{x}/r) - \hat{x}_1 \ . \tag{56}$$

Thus, the set of expressions (49)–(56) allows one to compute $b_2$ for an arbitrary x. Note that $b_2$ depends on the SNR and, consequently, may be *a priori* unknown since the SNR depends on the received signal power. Therefore, $b_2$ cannot be corrected by means of a permanent look-up correction table.

Figure 5 shows the signal-dependent bias $b_2$ versus deviation of the light spot. Inspection of Fig. 5 reveals that the signal-dependent bias is always negative, and an improvement of the SNR entails monotonous decrease of the bias magnitude for every x. Further, the magnitude of the signal-dependent bias monotonically increases as the light spot moves away from the QD center. Thus, the maximum bias magnitude is created when x = r.

While expressions (49)–(56) are useful for theoretical analysis, approximate formulas may be desired for practical applications. In what follows, several simple approximations are developed.

If the signal-to-noise ratio is large, then expression (25) holds true, expression (41) may be used, and (48) immediately yields

$$b_2 = \text{SNR}^{-1}\left[\left(\frac{S}{S_1} + \frac{S}{S_4}\right)\left(1 - \hat{x}_1\right) - \left(\frac{S}{S_2} + \frac{S}{S_3}\right)\left(1 + \hat{x}_1\right)\right] \ . \tag{57}$$

Expression (57) and Fig. 5 imply that the considered system possesses a signal- and position-dependent bias. When the light spot is located in the QD center, $\hat{x}_1 = 0$; in addition, $S_1 = S_2 = S_3 = S_4$, and $b_2 = 0$—this is a zero bias condition. However, when the light spot is located far from the QD center, a large negative bias is developed. As an example, consider a case when y = 0. Then $S_1 = S_4$, $S_2 = S_3$, and expression (57) yields

$$b_2 = SNR^{-1}\left[\frac{2S}{S_1} - \frac{2S}{S_2} - \left(\frac{2S}{S_1} + \frac{2S}{S_2}\right)\hat{x}_1\right] . \quad (58)$$

As x approaches r, $\hat{x}_1/r$ approaches unity (see Fig. 3), and, according to expression (58), $b_2$ approaches $-SNR^{-1}\cdot(4S/S_2)$. Since $S_2$ approaches zero at the same time, $|b_2|$ increases rapidly, while $b_2$ itself remains negative. Thus, $b_2$ "increases negatively," and the device underestimates deviation of the light spot for large x. Although the foregoing conclusion is qualitatively true, expression (58) cannot be used for quantitative evaluation of $b_2$ when x approaches r. The reason is that when $S_2$ approaches zero, expression (24) no longer holds true, and approximations (21), (22), (41), and (57) can no longer be used. For $y = 0$ and $x = r$, expressions (26) and (27) should be used in (31)–(34); as shown in Appendix A, the result is

$$b_2 = -5\sqrt{SNR} \text{ when } x = r . \quad (59)$$

Expression (59) is very important since it provides an approximate value of the *maximum* bias. Comparison of the values of $b_2$ given by expression (59) with those indicated in Fig. 5 shows that (59) provides an excellent accuracy (better than 3%) if SNR $\geq$ 30 dB. However, if SNR $<$ 30 dB, then expressions (49)–(56) should be used for bias evaluation. Note that $b_2$ is not at all negligible when $x = r$, even for relatively large SNR. For instance, the bias is equal to $-0.4$ (i.e., 40% of the light spot radius) if SNR = 20 dB; and the bias is equal to $-0.16$ (i.e., 16% of the light spot radius) if SNR = 30 dB. If system specifications demand lower bias, and SNR cannot be improved, then the measurement span must be restricted to a fraction of the light spot radius. If, e.g., the bias of 10% is allowed, then the measurement span must be restricted to 1/3 of the light spot radius when SNR = 20 dB (see Fig. 5).

### 3.6. Total system bias

Recall that the total system bias is defined by expression (3a). Therefore,

$$b = b_1 + b_2 = E\left(\frac{\hat{x}}{r}\right) - \frac{x}{r} , \quad (60)$$

as follows from the comparison of expressions (3a), (47), and (48). Total system bias b versus deviation of the light spot is shown in Fig. 6 (computed using expressions (47), (49)–(56), and (60)).

Inspection of Fig. 6 reveals that improvement of SNR entails monotonous decrease of the system bias for large x ($x \simeq r$); however, for $x \simeq 0.7r$, a positive bias is developed for large SNR, instead of the negative bias for small SNR. The reason is that as the SNR increases, the signal-dependent bias decreases, and the total bias approaches the systematic error given by expression (47). Hence, instead of the *negative* signal-dependent bias, one obtains a *positive* systematic error (see Fig. 4). If the systematic error is cancelled (i.e., by means of a look-up correction table), then $b_2 = b$, and the system bias may be found from Fig. 5.

We proceed now to the evaluation of the estimation variance.

### 3.7. Estimation variance

It follows from expression (39) and definition (3b) that

$$\text{var}\,\hat{x} = \text{var}\,\Delta/[E(\Sigma)]^2 = \sum_{k=1}^{4} \text{var}\, r_k \Big/ \left(\sum_{k=1}^{4} \bar{r}_k\right)^2 . \quad (61)$$

If expression (25) holds true, then (21) and (22) may be substituted in (61), yielding the following result (we have used expression (14) for $\sigma_k^2$):

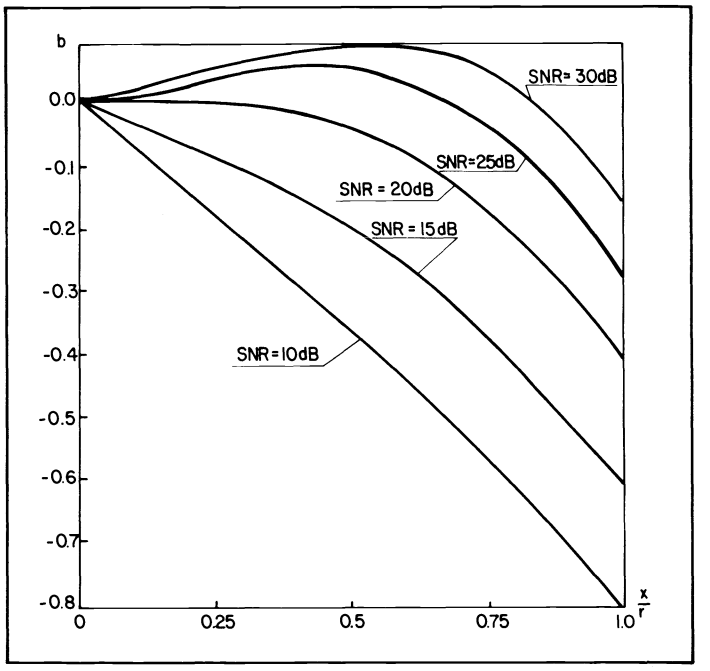


**Fig. 6. Total system bias versus deviation of the light spot.**

$$\text{var}\,\hat{x} = SNR^{-1}\,\frac{\sum_{k=1}^{4}(1-\beta_k)}{\left[\sum_{k=1}^{4}(1+\beta_k)S_k/S\right]^2} . \quad (62)$$

Now, let us consider two special cases: (a) the light spot is located in the center of the QD, and (b) the light spot is located at the end of the measurement span ($x = r$).

If the light spot is located in the center of the QD, then $x = y = 0$, $S_k/S = 1/4$, and $\beta_k = 8/SNR$ [see expression (24)]; hence, expression (62) yields

$$\text{var}\,\hat{x} = SNR^{-1}\cdot 4\cdot\left(1 - \frac{8}{SNR}\right)/(1 + 8/SNR)^2 . \quad (63)$$

For very high signal-to-noise ratios, SNR $\gg$ 8, and expression (63) yields

$$\text{var}\,\hat{x} = 4\cdot SNR^{-1} . \quad (64)$$

If the light spot is located at the point ($x = r$, $y = 0$), then $S_1 = S_4 = 0.5\cdot S$, and $S_2 = S_3 = 0$; hence, expression (25) does not hold true, and (62) cannot be used. In this case, we substitute expressions (26) and (27) in (61) with the following result:

$$\text{var}\,\hat{x} = \frac{1.5\,\sigma_2^2 + 2\sigma_1^2\left(1 - \frac{2}{SNR}\right)}{\left[\sigma_2\sqrt{\frac{\pi}{2}} + 2a_1\left(1 + \frac{2}{SNR}\right)\right]^2} , \quad (65)$$

where

$$\sigma_1^2 = B\left[N_t + 2q(0.5\,\bar{i}_S + 0.5\,\bar{i}_S m + \bar{i}_d + \bar{i}_b)\right] , \quad (66)$$

$$\sigma_2^2 = B\left[N_t + 2q(\bar{i}_d + \bar{i}_b)\right] , \quad (67)$$

and

$$a_1 = 0.5\bar{i}_S m \ . \tag{68}$$

For high signal-to-noise ratios,

$$\text{var}\,\hat{x} \simeq \frac{1.5\sigma_2^2 + 2\sigma_1^2}{(\bar{i}_S m)^2} \leq \text{SNR}^{-1} \cdot 3.5 \ . \tag{69}$$

Comparing expression (69) with (64), we note that the estimation variance at the end of the measurement span is nearly the same as at the QD center. Thus, the main consequence of the deviation of the light spot from the QD center is the increase of the estimation bias, rather than a change of the estimation variance.

## 4. CONCLUSIONS

In this paper we have theoretically evaluated performance of the QD-based laser tracking system. Measurement span, estimation bias, and estimation variance were analyzed, with the emphasis on the quantitative evaluation of the estimation bias and variance. The main findings of our study may be summarized as follows. The measurement span does not exceed the radius of the light spot r; if system specifications restrict estimation bias, then the measurement span must be limited even further, to a fraction of r. If, for instance, the bias is restricted to 10% of r and SNR is equal to 20 dB, then the measurement span should not exceed r/3. Estimation bias contains two components: systematic error (signal-independent bias, which exists even for infinitely large SNR), and signal-dependent bias. The systematic error is rather large (up to 11.5% of the light spot radius); fortunately, it may be cancelled by means of a permanent look-up correction table stored in a ROM. Signal-dependent bias cannot be cancelled with the same technique since it depends on the *a priori* unknown signal intensity. Signal-dependent bias decreases when the SNR increases, at a rate proportional to $\sqrt{\text{SNR}}$; it increases rapidly when the light spot approaches the end of the measurement span. Estimation variance was also evaluated. It was found to decrease when the SNR increases, at a rate roughly proportional to SNR. Estimation variance remains approximately constant as the light spot moves over the measurement span. Thus, the main consequence of the deviation of the light spot from the QD center is the increase of the estimation bias, rather than a change of the estimation variance.

## 5. ACKNOWLEDGMENT

The author wishes to thank the reviewers of this paper for their helpful comments.

## 6. APPENDIX A

In this Appendix, we evaluate the signal-dependent bias for a case when $x = r$ and $y = 0$ (see Fig. 2). Substituting expressions (21) and (26) in (40) yields

$$E(\hat{x}) = r \cdot \frac{a_1(1+\beta_1) - \sigma_2\sqrt{\pi/2}}{a_1(1+\beta_1) + \sigma_2\sqrt{\pi/2}} \ . \tag{A1}$$

Substituting expression (A1) in (48), we obtain

$$b_2 = \frac{1+\beta_1 - \sigma_2\sqrt{\pi/2}\,a_1}{1+\beta_1+\sigma_2\sqrt{\pi/2}\,a_1} - 1 = -2\sqrt{\pi/2}\,\frac{\sigma_2}{a_1} + \text{higher order terms} \ . \tag{A2}$$

Substituting $a_1 = 0.5\,\bar{i}_S m$ and $\sigma_2 = B[N_t + 2q(\bar{i}_d + \bar{i}_b)]$ in (A2), then neglecting higher order terms, we obtain

$$b_2 = -\frac{4\sqrt{\pi/2}}{\sqrt{\widetilde{\text{SNR}}}} \simeq -5\sqrt{\widetilde{\text{SNR}}} \ , \tag{A3}$$

where

$$\widetilde{\text{SNR}} \triangleq \bar{i}_S^2 m^2 / B[N_t + 2q(\bar{i}_d + \bar{i}_b)] \ . \tag{A4}$$

If

$$2q\bar{i}_S(1+m) \ll N_t + 2q(\bar{i}_d + \bar{i}_b) \ , \tag{A5}$$

then $\widetilde{\text{SNR}} \simeq \text{SNR}$ [see expression (24a)], and (A3) yields

$$b_2 = -5\sqrt{\text{SNR}} \ , \tag{A6}$$

which is the desired result.

## 7. APPENDIX B: TABLE OF SYMBOLS

*Symbols of English Alphabet*

| | |
|---|---|
| $a_k$ | amplitude of the ac signal current of the k-th detector (k = 1,2,3,4); |
| $b\hat{x}$, or simply b | total estimation bias in the x-direction; |
| $b_1$ | systematic error, or signal-independent bias; |
| $b_2$ | signal-dependent bias; |
| B | bandwidth of electronic filters; |
| d | diameter of the light spot; |
| D | diameter of the quadrant detector; |
| $E(\cdot)$ | mathematical expectation of $(\cdot)$; |
| $f_c$ | system focal length; |
| $G_k \triangleq a_k^2/4\sigma_k^2$; | |
| h | Planck constant; |
| $i_k$ | current of the k-th detector (k = 1,2,3,4); |
| $\bar{i}_{sk}$ | average signal current of the k-th detector (k = 1,2,3,4); |
| $\bar{i}_{nk}$ | average noise current (dc) of the k-th detector (k = 1,2,3,4); |
| $i_{nk}$ | zero-mean random process at the output of the k-th detector (k = 1,2,3,4); |
| $\bar{i}_s$ | total signal current of the quadrant detector; |
| $i_{fk}$ | filtered version of $i_k$; |
| $i_{fnk}$ | filtered version of $i_{nk}$; |
| $\bar{i}_d$ | detector dark current; |
| $\bar{i}_b$ | detector current due to background radiation; |
| I | irradiance of the signal field [W/cm$^2$]; |
| $I_0$ | nominal light irradiance (average value of I); |
| $I_0(\cdot)$ | modified Bessel function of the first kind of zero order; |
| $I_1(\cdot)$ | modified Bessel function of the first kind of first order; |
| k | index; k = 1,2,3,4; |
| m | depth of intensity modulation of the light signal; |
| M | measurement span; |
| $N_k$ | power spectral density of $i_{nk}$; |

$N_t$ power spectral density of the thermal noise due to both the photodetector and the associated electronic circuits;

$p(\cdot)$ probability density function of $(\cdot)$;

$q$ electron charge;

$r$ radius of the light spot;

$r_k$ envelope of $i_{fk}$;

$\bar{r}_k$ expectation of $r_k$;

$\bar{r}_k^! \triangleq \bar{r}_k / \sigma_k \sqrt{\pi/2}$ ;

ran random zero-mean variable;

$S$ total area of the light spot;

$S^! \triangleq S/r^2$ normalized value of S;

$S_k$ area of the light spot on the surface of the k-th detector (k = 1,2,3,4);

SNR signal-to-noise ratio [formal definition is given by expression (24a)];

$\widetilde{SNR}$ approximate value of SNR [formal definition is given by expression (A4)];

var variance;

$x$ horizontal coordinate of the light spot center (see Fig. 2);

$\hat{x}$ estimated value of x;

$\hat{x}_1 \triangleq [(S_1 + S_4) - (S_2 + S_3)]/S$ signal-independent component of $E(\hat{x})$;

$y$ vertical coordinate of the light spot center (see Fig. 2);

$\hat{y}$ estimated value of y;

$y(\cdot)$ photodetector angle response.

*Symbols of Greek Alphabet*

$\alpha$ angle identified in Fig. 2;

$\beta_k \triangleq \sigma_k^2 / 2a_k^2$, k = 1,2,3,4;

$\Delta \triangleq r_1 + r_4 - r_2 - r_3$;

$\epsilon$ higher order terms in expression (41);

$\theta$ angle of incidence of light on the detector surface;

$\theta_x$, $\theta_y$ arrival angles of the optical signal beam measured from the system optical axis;

$\nu$ light frequency;

$\sigma_k^2 \triangleq$ var $i_{fnk}$, where k = 1,2,3,4,;

$\Sigma \triangleq r_1 + r_2 + r_3 + r_4$;

$\omega$ modulation frequency.

## 8. REFERENCES


1. P. A. Forrester and K. F. Hulme, Opt. and Quantum Electron. 13, 259(1981).
2. E. V. Browell, Opt. Eng., 21(1), 128(1982).
3. J. H. Shapiro, B. A. Capron, and R. C. Harney, Appl. Opt. 20(19), 3292(1981).
4. M. I. Skolnik, *Introduction to Radar Systems,* McGraw Hill, New York (1980).
5. R. C. Harney and R. J. Hull, Proc. SPIE, 227, 162(1980).
6. P. M. Salomon, Opt. Eng. 20(1), 135(1981).
7. H. E. Rauch, W. I. Futterman, and D. B. Kemmer, Opt. Eng. 20(1), 103(1981).
8. W. L. Wolfe, Ed., *Handbook of Military Infrared Technology,* Chap. 18. 7, Office of Naval Research, Department of the Navy, Washington, D.C. (1965).
9. L. G. Kazovsky, IEEE Trans. Instrum. Meas. IM-31(1), 60(1982).
10. R. M. Gagliardi and S. Karp, *Optical Communications,* Wiley, New York (1976).
11. L. G. Kazovsky, *Transmission of Information in the Optical Waveband,* Wiley, New York (1978).
12. A. Papoulis, *Probability, Random Variables and Stochastic Processes,* p. 499, McGraw Hill, New York (1965).